DYNAMIC APERTURE EVALUATION FOR THE HADRON STORAGE RING OF ELECTRON-ION COLLIDER*

Y. Luo†, J. S. Berg, X. Gu, H. Lovelace III, M. Blaskiewicz, W. Fischer, C. Montag, R. Palmer,
S. Peggs, V. Ptitsyn, F. Willeke, H. Witte, D. Xu, Brookhaven National Laboratory, Upton, NY, USA
Y. Hao, Facility for Rare Isotope Beams, Michigan State University, East Lansing, MI, USA
J. Qiang, Lawrence Berkeley National Laboratory, Berkeley, CA, USA
E. Nisson, H. Huang, V. Morozov, T. Satogata
Thomas Jefferson National Accelerator Facility, Newport News, VI, USA

Abstract

The Electron-Ion Collider (EIC) is aiming at a design luminosity of 1×10^{34} cm^{-2}sec^{-1} with collision with 10 GeV electrons and 275 GeV protons. To maintain such a high luminosity, both beams need an acceptable beam lifetime in presence of beam-beam interaction. For this purpose, we carried out weak-strong element-by-element particle tracking to evaluate the long-term dynamic aperture for the Hadron Storage Ring (HSR) lattice. We improved our simulation code SimTrack to treat some new lattice design features, such as crossing collision with crab cavities, a radially offset on-momentum orbits, etc. In this article, we present the preliminary dynamic aperture calculation results with crossing collision with crab cavities and magnetic field errors in interaction region.

INTRODUCTION

In the Electron-Ion Collider (EIC) design, there are several different collision configurations that have different combinations of electron and ion beam energies [1]. In the following, we will only discuss collisions between 10 GeV electrons and 275 GeV protons, which is the configuration with the highest luminosity, reaching 1×10^{34} cm^{-2}sec^{-1}. This combination also requires the highest beam-beam parameter for both the proton and electron beams among all configurations [1].

The Hadron storage ring (HSR) of EIC will re-use the existing RHIC arcs. Based on RHIC operational experience, calculated 10^6 turn dynamic aperture with beam-beam interaction and IR nonlinear field errors should be larger than 5 σ with 3 $(dp/p_0)_{rms}$ to guarantee an acceptable beam lifetime at physics store. The beam-beam parameters for the proton beam in HSR and in RHIC are almost same, around 0.015. Therefore, we require HSR should have a larger dynamic aperture than 5 σ with 3 $(dp/p_0)_{rms}$. For HSR, the RMS relative momentum spread is $(dp/p_0)_{rms} = 6 \times 10^{-4}$.

Table 1 lists the beam-beam related design parameters presented in EIC Conceptual Design Report (CDR) for the collision with 10 GeV electrons and 275 GeV protons. The proton ring working point is $((0.228, 0.210)$. Proton's (β_x^*, β_y^*) at IP are (80, 7.2) cm. They were determined by beam-beam studies with strong-strong and weak-strong simulations [2].

Table 1: Beam-beam Related Machine and Beam Parameters for 10 GeV Electron and 275 GeV Proton Collision in EIC

Quantity	Unit	Proton	Electron
Beam energy	GeV	275	10
Bunch intensity	10^{11}	0.668	1.72
(β_x^*, β_y^*) at IP	cm	(80, 7.2)	(55, 5.6)
Beam sizes at IP	μm	(95, 8.5)	
Bunch length	cm	6	2
Energy spread	10^{-4}	6.6	5.5
Transverse tunes		(0.228, 0.210)	(0.08, 0.06)
Longitudinal tune		0.01	0.069

SIMULATION SETUP AND LATTICE DESIGN

Crossing Colliison with Crab Cavities

There are a few new features for HSR than RHIC. First, EIC adopts a full crossing angle of 25 mrad at IP. To compensate the geometric luminosity loss due to the crossing angle, crab cavities are used to tilt the proton and electron bunches in the $x - z$ plane by half of the full crossing angle to restore head-on collision condition. For EIC, local crabbing scheme is adopted.

For each ring, two sets of crab cavities are installed on both sides of IP, with an ideal horizontal betatron phase advance $\pi/2$ between IP and crab cavities. The voltage of the crab cavity is given by

$$\hat{V}_{RF} = -\frac{cE_s}{4\pi f_{RF}\sqrt{\beta_x^*\beta_{x,cc}}}\theta_c. \tag{1}$$

Here c is the speed of light, E_s is the particle energy in eV, f_{RF} is the crab cavity frequency, and θ_c is the full crossing angle. β_x^* and $\beta_{x,cc}$ are the horizontal β functions at the IP and the crab cavity, respectively. To reduce the requirement for the crab cavities in HSR, $\beta_{x,cc}$ at crab cavities reaches 1300 m. From beam-beam simulation study, the orbits , the horizontal dispersion D_x, and its derivative D_x' at crab cavities should be close to zero as possible.

For dynamic aperture calculation, we assume that the electron bunch is rigid and it is perfectly crabbed. To simulate crossing collision, we install crab cavities into HSR lattice.

MC1: Circular and Linear Colliders

A19 Electron-Hadron Colliders

At IP, Lorentz Boost is used to transfer the coordinates of protons from laboratory coordinate frame to a head-on collision frame, where beam-beam kicks are applied. The electron bunch is split into 5 longitudinal slides.

Radial Shift Orbit

To match revolution frequency of Electron Storage Ring (ESR), HSR needs to be able to adjust its pathlength, which is achieved with radial shift orbit in arcs [3]. The required pathlength change and average radial orbit shift vary at different collision energies. The radial shift orbit is created with a field deviation from the nominal design value by $\Delta B/B_0$ to arc bending dipoles. The design orbit should always be centered in all IRs.

With radial shift orbit, on-momentum design orbit will not go through center of arc main dipoles as most accelerators. The phases of RF cavities, crab cavities should be synchronized with on-momentum particle. Also, due to the large radial orbit shift for some collision modes, we need to pay attention to the impact of magnetic field errors in arc magnets, which is ignored in RHIC dynamic aperture calculation.

Lattice Design

Figure 1 shows the off-momentum tunes for the current HSR lattice design. The horizontal axis is the relative momentum deviation dp/p_0 up to 20×10^{-4}, which is about $3\ (dp/p_0)_{rms}$. So far we only use two sextupole families to correct the first order chromaticities to 1. The second order chromacticies are (700, -400) which are a factor 2-3 smaller than those from RHIC. There are totally 24 independent sextupole families in HSR arcs. It is possible to use multi-families for further chromatic effect correction.
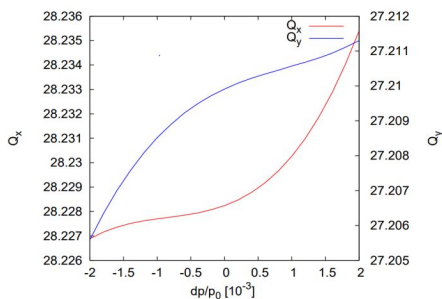

Figure 1: Off-momentum tunes with current HSR lattice design.

DYNAMIC APERTURE WITH BEAM-BEAM

Without Magnetic Field Errors

First we calculate and compare the proton dynamic aperture without any field error in the HSR lattice. Dynamic aperture is calculated with a 6-d symplectic particle tracking code SimTrack [4], which has been used for RHIC dynamic aperture calculation in the past ten more years. For each

study condition, test particles are launched in the first quadrant of phase space $(x/\sigma_x, y/\sigma_y)$ in 5 equal distance phase angles. Test particles are tracked up to 1 million turns. We focus on comparing the minimum dynamic aperture among those 5 phase angles. More phase angles can be added in future studies.

Figure 2 shows the dynamic aperture in 5 phase angles with head-on and crossing collision with crab cavities. The proton's relative momentum deviation is 20×10^{-4}. In the plot, the dynamic aperture is larger close to 90 degrees in phase space. The reason is that the design vertical RMS beam size is 10 times smaller than the horizontal one. Without magnetic field error, the minimum dynamic aperture among 5 phase angles is about 20 σ with head-on and crabbed collisions.
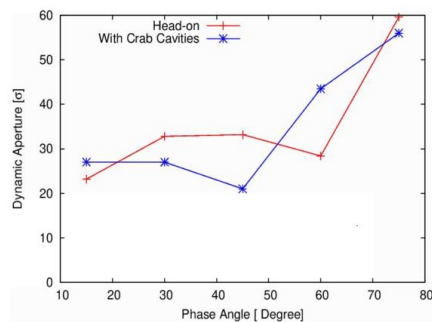

Figure 2: Dynamic aperture without IR magnetic field errors: head-on and crabbed collisions.

With Magnetic Field Errors

Based on RHIC experience, IR magnetic field errors play an important role in dynamic aperture reduction. At the this point, we artificially assign high order field errors to all IR dipoles and quadruples within 160 m from IP. The goal of this study is to exam the impact of IR field errors on dynamic aperture and to determine their tolerances.

Magnet field errors are defined as

$$(B_y L) + i(B_x L) = \\ B(R_r)L \left[10^{-4} \sum_{n=0}^{N_{max}} (b_n + ia_n) \frac{(x+iy)^n}{R_r^n} \right]. \quad (2)$$

Here L is the magnet length, R_r is the reference radius where the magnetic field is measured, $B(R_r)$ is the main field at R_r, b_n and a_n are the normal and skew magnetic components. For dipoles, $b_0 = 10^4$. For upright quadrupoles, $b_1 = 10^4$. Components other than the design ones are field errors.

Both systematic and random field errors can be assigned in the tracking code. Here we focus on the random field errors. The random error distribution can be Gaussian or uniform. In the following dynamic aperture calculation, we used uniform distribution. For each condition, 10 sets of random field errors are used in current studies. For the first tests, we do not distinguish field errors for different IR magnets and different components of field errors. The reference radius is set to 60 mm for all IR dipoles and 40 mm for all IR

MC1: Circular and Linear Colliders

A19 Electron-Hadron Colliders

quadrupoles. Tracking with more realistic reference radius is planned.

After installing magnetic field errors, we noticed sizable changes in the orbits and tunes. Orbit offsets at beam-beam interaction point and crab cavities should be avoided. We install 4 local beam position monitors and 4 dipole orbit correctors in each transverse plane around IP to correct the orbits at IP and crab cavities. After that, we re-match the lattice tunes to their design values without beam-beam. We then install beam-beam kick at IP and crab cavities. They are not included during above orbit and tune corrections due to IR magnetic field errors.

Figure 3 shows the dynamic aperture with beam-beam and with IR field errors. The dynamic aperture is the averaged dynamic aperture among 10 seeds. The RMS variation of calculated dynamic aperture is about 1 σ for all following cases. With 1 unit of field errors, the dynamic aperture with head-on collision drops to 9 σ, while the dynamic aperture with crossing collision and crab cavities drops to 6 σ. Currently we are looking for the reasons for the difference in the dynamic aperture between head-on and crabbed collisions. This discrepancy is not seen without IR field errors. It may come from not exact 90 degrees phase advances between IP and crab cavities. For current lattice design, the phase advances are about 2-4 degrees off 90 degrees. The impact of synchro-betatron motion and second harmonic cavities to dynamic aperture are to be studied.
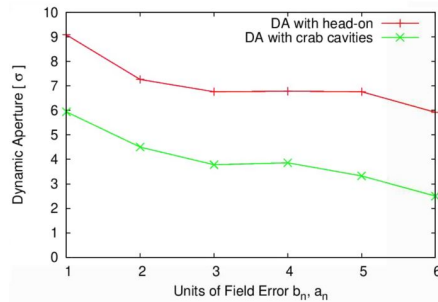

Figure 3: Dynamic aperture with IR field errors: head-on and crabbed collisions.

Next we carry out some contrast comparisons for IR field errors, as shown in Fig. 4. First we compare dynamic aperture with field errors assigned to IR magnets within 160m (red curve) and 80m (green curve) from IP. In the plot, the horizontal axis is units of IR field errors and vertical axis is the averaged calculated dynamic aperture from 10 seeds. There is no big improvement in dynamic aperture when we assign field errors to magnets within 80 m instead of 160 m from IP. This means that the important field errors to dynamic aperture are those closer to IP.

Then we exclude sextupole field errors (blue curve) from IR magnets. Compared to the green curve in the plot, the dynamic aperture improves marginally. This means that the sextupole component of field errors may not be the predominate field error for HSR dynamic aperture. Impacts from other component of field errors should be focused too.
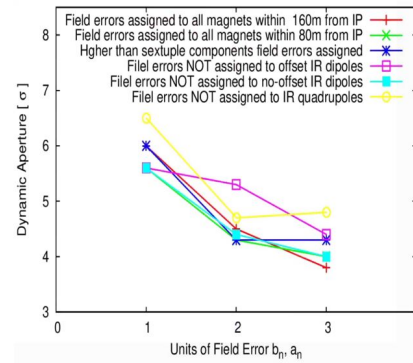

Figure 4: Dynamic aperture comparison with different IR field error assignment scenarios.

For the last comparison, we intentionally do not assign field errors to IR dipoles without orbit offset, IR dipoles with orbit offset, and IR quadruopoles. From Fig. 4, dynamic aperture increases when field errors not assigned to quadrupoles (yellow curve) and offset dipoles (purple curve). This means that field errors of IR quadrupoles and IR offset dipoles are more important to dynamic aperture reduction. More detailed studies about individual IR magnet's impact on dynamic aperture are planned.

SUMMARY

In this article, with a weak-strong beam-beam interaction model, we calculated the proton dynamic aperture in HSR with collision between 10 GeV electrons and 275 GeV protons. Preliminary dynamic aperture calculation shows that dynamic aperture with beam-beam and without IR field errors is about 20 σ. With artificial random IR field errors of 1 unit, dynamic aperture with beam-beam drops to 9 σ with head-on collision and drops to 6 σ with crossing collision with crab cavities. We are looking for the reason for this difference between them. We also found that field errors in IR quadrupoles and offset dipoles play a bigger role in dynamic aperture reduction. We will continue studying the impact from individual magnet and individual field component with more realistic magnet measurement reference radius to determine the tolerances of IR magnetic field errors.

REFERENCES

[1] C. Montag *et al.*, "Design Status Update of the Electron-Ion Collider", presented at the 12th Int. Particle Accelerator Conf. (IPAC'21), Campinas, Brazil, May 2021, paper WEPAB005, this conference.

[2] Y. Luo *et al.*, "Beam-Beam Related Design Parameter Optimization for the Electron-Ion Collider", presented at the 12th Int. Particle Accelerator Conf. (IPAC'21), Campinas, Brazil, May 2021, paper THPAB028, this conference.

[3] S. Peggs *et al.*, "Large Radial Shifts in the EIC Hadron Storage Ring", presented at the 12th Int. Particle Accelerator Conf. (IPAC'21), Campinas, Brazil, May 2021, paper TUPAB042, this conference.

[4] Y. Luo, "SimTrack: A compact c++ code for particle orbit and spin tracking in accelerators", *Nucl. Instrum. and Methods A*, vol. 801, pp. 95-103, Nov. 2015. doi:10.1016/j.nima.2015.08.014